Testing and Reconciling Stress Drop and Attenuation Models for Southern California

Technical Report for SCEC Award # 17041

Investigators: Rachel Abercrombie (BU) and Peter Shearer (UCSD)

The objective of this work is to improve the quality and reliability of stress drop measurements in southern California. The main focus of our work has been to compare the complementary approaches of the two PIs to determine the sources of consistency and discrepancy between stress drop measurements. Are the main discrepancies between the two approaches a consequence of the different methods of resolving the source spectra and modeling them, or are they mainly a consequence of the limited quality and quantity of the data? Can we use these results to improve the quantification of uncertainties in stress drop estimates? Previously, we investigated, developed and adapted the two different approaches and applied them to a cluster of events near Landers. In the current award period, we focus on comparing in detail the two approaches, using a small number of selected events, to determine the main sources of uncertainty. We then perform initial synthetic modeling to investigate further the trade-offs within the methods.

Motivation and Relation to the SCEC Goals

Small earthquakes dominate earthquake catalogs, but only their locations and magnitudes are routinely determined. To understand the evolving stress state within southern California, a priority of SCEC4 and SCEC5, as well as earthquake physics and scaling relations, we need to go beyond this. Earthquake stress drop, proportional to the slip divided by the length scale of rupture, is a basic property of earthquakes and is fundamental to the physics of the source and its energy budget [*Kanamori and Brodsky*, 2004]. It is often estimated by measuring the corner frequency and assuming a simplified theoretical model of rupture [e.g., *Brune*, 1970; *Madariaga*, 1976; *Kaneko and Shearer*, 2014, 2015]. Knowledge of the true variability of stress drop is essential to strong ground motion modeling and prediction [e.g. *Cotton et al.*, 2013; *Baltay et al*., 2017]. The large number of stress drop studies attest to its importance, but their widely varying results (~0.1 to 100 MPa), the large uncertainties (when calculated), and the ongoing controversy of whether stress drop changes with moment are evidence for how hard it is to calculate reliably [e.g., *Abercrombie* et al., 2017a; *Abercrombie and Rice*, 2005; *Shearer et al*., 2006; *Pacor et al.*, 2016; *Kwiatek et al.*, 2011; Trugman *et al.*, 2017b]. This uncertainty severely limits the use of stress drop studies in (a) quantifying the spatial heterogeneity of the stress state over a wide range of scales [e.g., *Hauksson*, 2014], (b) predicting strong ground motion [e.g., *Baltay et al*., 2013, 2017], and (c) discriminating induced seismicity [e.g., *Huang et al.*, 2016; *Zhang et al*., 2016], all priorities of SCEC4 and SCEC5.

The main problem in calculating earthquake stress drop is how to separate source and path effects in band-limited signals and so measure corner frequency reliably. The fact that stress drop is proportional to the cube of the corner frequency only exacerbates the problem. Various forms of empirical Green's function (EGF) analysis, in which the seismogram of a co-located small earthquake is used to represent the path effects in a larger earthquake recording, should decrease the trade-offs inherent in extracting the source spectrum [e.g., *Kwiatek et al*., 2014]. If multiple earthquakes, recorded at multiple stations, are combined then it is possible to invert for both source parameters (constant for each event) and path effects (constant for individual paths), e.g., *Oth et al*. [2011]. Most analyses, however, concentrate on either source [e.g., *Shearer et al.*, 2006; *Abercrombie et al.*, 2017a] or attenuation [e.g., *Hauksson and Shearer*, 2006], often with simplifying assumptions, and do not test for the self-consistency of the resulting models. An improved model of attenuation is a priority of the GM group in SCEC4 and SCEC5.

Initial Stress Drop Estimates

Our analysis focuses on detailed comparisons of two different approaches for estimating earthquake stress drops from P-wave spectra: (1) the spectral decomposition and global EGF method of *Shearer et al.* [2006], a large-scale, automated approach involving stacking and averaging spectra to obtain parameters for large catalogs of events; and (2) the traditional empirical Green's function (EGF) method of *Abercrombie et al.* [2017a], a smaller-scale approach that attempts to obtain optimal results for a small number of the best-recorded earthquakes. We improved and developed these methods in previous SCEC and related work [see *Trugman and Shearer*, 2017 and *Abercrombie et al.*, 2017a], and applied them to two test regions with dense seismicity, one near the Landers earthquake epicenter and one around the Cajon Pass borehole, in which previous results predict spatial variability in both earthquake stress drops and attenuation. We found varying degrees of consistency, as shown in Figure 2, and selected some well-recorded events for detailed comparisons.

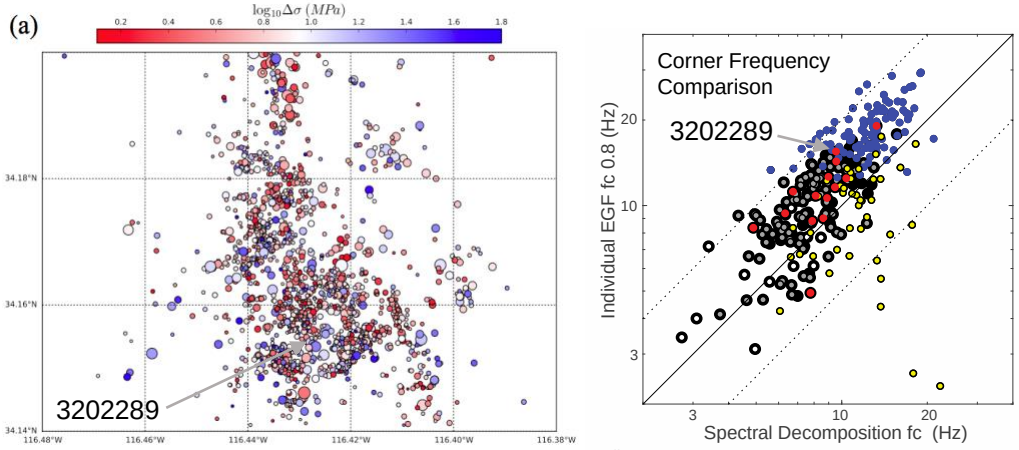

Figure 1. (a) Location of earthquakes in Landers test region, showing stress drop results for 1709 events from spectral decomposition without enforced self-similarity. (b) Comparison of stress drop estimates from spectral decomposition with individual event based EGF for the largest 950 events. The yellow and blue points are the least well constrained in the individual event based EGF. The red are the highest quality ratios, well fit by the simple circular source model; the white points are ratios of the same quality that exhibit spectral complexity. Event 3202289 (see Figure 2) is flagged.

Detailed Comparison of Individual Events

We selected seven events for detailed analysis. They are from the highest quality ratios in the individual EGF approach and include both simple and more complex spectral shapes. The steps of our comparison are outlined below. For both approaches the first step is to calculate the raw spectra. Then for the spectral decomposition, all the spectra at all stations for each event are stacked to produce an event spectrum which is then used in the ensuing analysis. For the individual EGF approach, the spectral ratio of each event-EGF pair is calculated individually for each station. For each target event, these ratios are then stacked to produce an event average (used here) and also averages by EGF and by station. The former is used to check for anomalous EGFs, and the latter to reveal azimuthal variations consistent with rupture propagation or complexity [e.g., *Abercrombie et al.*, 2017b].

1. We compare some raw spectra from individual events at individual stations and find no significant differences in our spectral calculations.

2. We select the spectra calculated for the spectral decomposition approach and use them to produce the same ratios calculated in the individual EGF approach. We investigate how the exact choice of stations and signal-to-noise criteria affect the average per-event ratios, and find that these choices have only minimal effect (Figure 2). For this event the EGF selection also appears to have negligible effect between the two methods.
3. Hence, we proceed by comparing the ratios of the relevant event spectra from the spectral decomposition with the individual EGF average spectral rations, as this is much simpler. Comparison of the event spectral ratios from the spectral decomposition shows good agreement with the individual EGF approach for all but one event. (Figure 3).

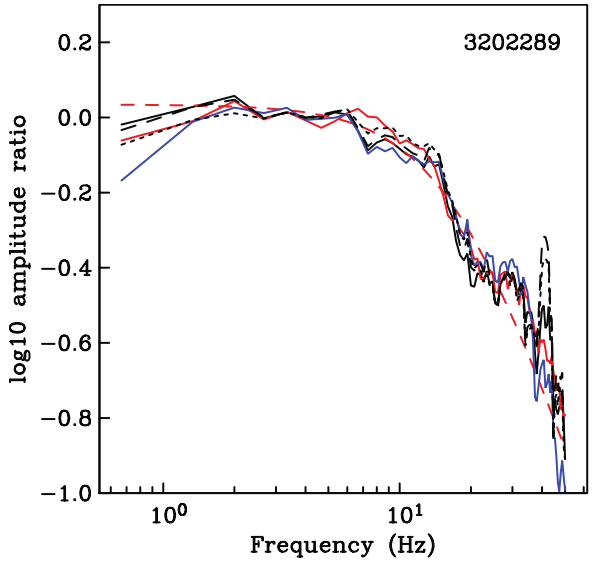

Figure 2. Stacked spectral ratios between M2.8 target event 3202289 and 241 EGF events for various STN criteria, and station selections. Solid black: stack of spectral ratios for all common stations between the target and EGF events, using the spectral decomposition analysis STN criteria. Solid Red: stack of spectral ratios of all event terms between the target and EGF events - event terms from spectral decomposition of the entire data set (5000 events). The other lines show other STN and EGF event choices and the short dashed lines show theoretical model fits. Note all the curves agree well.

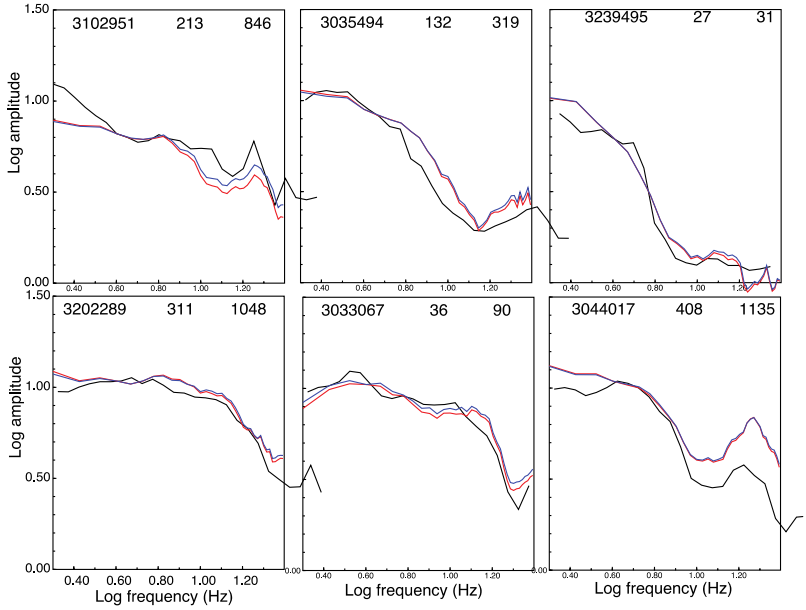

Figure 3. Source spectral ratio comparison for 6 example events, showing spectra from individual event EGF (black), spectral decomposition ratios for target event with same set of EGFs (but not necessarily same stations), equal weighting per EGF (red) and EGFs weighted by number of stations in individual EGF ratios (blue). The titles show the target event ID, the number of EGFs and the total number of spectral ratios.

Results of Spectral Comparison

Our detailed comparison of the spectral ratios obtained by the two different approaches shows that they are generally very similar, and the calculation of the spectra and ratios is unlikely to be the source of significant discrepancies between the methods. Thus, the greatest source of differences in the corner-frequency estimates between the two methods is likely due to the model fitting. In order to investigate how the model fitting affects the results, we compare: (a) results from fitting a global EGF function to all the event terms in the spectral decomposition, to (b) fitting the target to EGF event ratios directly as in most EGF approaches.

Figure 4 shows the results of fitting the source spectrum of event 3202289, and the stack of 241 highly correlated EGFs used in the individual EGF analysis, all corrected with the global EGF from spectral decomposition. We fit the ratio of the main event to the EGF stack as in spectral ratio EGF approaches. The fits to the target and EGF events do not match the ratio, nor the fit to the ratio. The inferred global EGF from the ratio fit is not a good match to the whole data set used in the spectral decomposition. Overall, this results in a large mismatch in the estimated corner frequency for the target event (7.5 vs. 14 Hz).

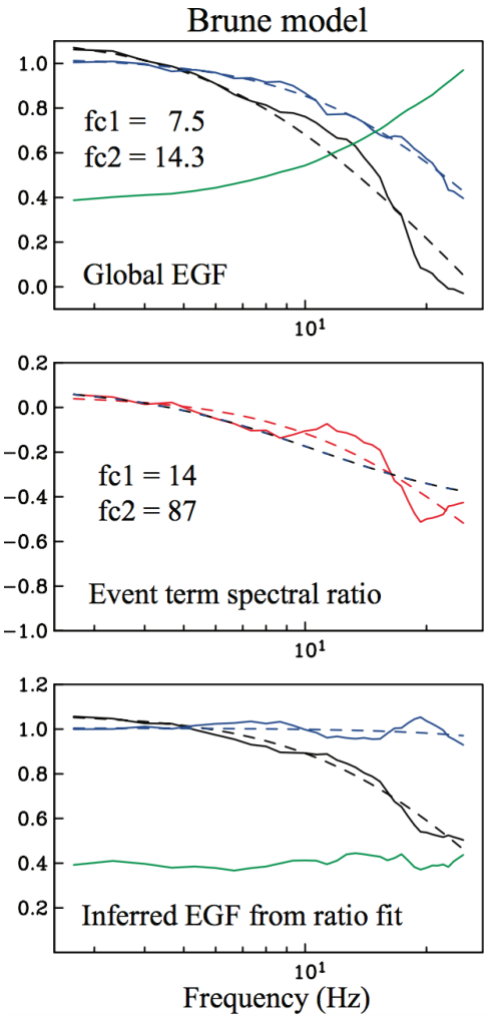

Figure 4. Corner frequency fits for event 3202289. For comparison, all spectra are shifted to agree at low frequency. Top: event terms for the target (black) and stack of 241 EGFs (blue) corrected for the global EGF function (green). The individual fits for the target event corner frequency (fc1) and EGF stack corner frequency (fc2) are shown as dashed lines. Middle: The difference (spectral ratio) between the target and EGF event stack is shown in red. The red dashed line shows the best-fitting model when both fc1 and f2 are allowed to vary. The black/blue dashed line shows the prediction of the individual fits to the EGF-corrected spectra in the top panel. Bottom: Estimated target and EGF event spectra from the best-fitting fc1 and fc2 values from the ratio approach in the middle panel. The inferred global EGF is shown as the green line, the fits to the data are shown as the dashed lines.

Why does this difference occur? One reason is that the "bump" in the target event spectrum near 10 to 15 Hz prevents a perfect fit to the model. The spectral ratio fitting method can reduce the misfit by shifting the corner frequency of the EGF event stack to a very high value. This results in a very flat inferred EGF (green curve in lower panel). In contrast, the global EGF fitting approach does not have as many degrees of freedom because its EGF must fit the entire data set in a self-consistent manner. Thus, although its predicted fit to the spectral ratio stack (middle panel) is not as good, its corner frequency estimate is arguably more reliable because its inferred EGF is more realistic, i.e., it does not require a very high average corner frequency for the EGF events.

Synthetic Modeling of Parameter Resolution

To explore these issues in more detail, we have begun conducting experiments using synthetic spectra. This work is also motivated by *Trugman and Shearer* [2017], who found that although a systematic increase in stress drop with earthquake moment gave the best fit to the data, there are strong trade-offs between scaling, average stress drop, and the high-frequency fall-off rate in several regions of southern California. We find the same issue for the Landers test region considered here. Our preliminary synthetic modeling work shows that with the magnitude distribution and frequency range of data available for the Landers region, we are unable to constrain the trade-off between self-similarity and high-frequency spectral shape.

The *Shearer et al.* [2006] stress drop study for southern California enforced a self-similar Brune model with a high-frequency (HF) fall-off rate, n, of 2 and obtained reasonable fits to moment-binned spectra stacks. However, as shown by *Trugman and Shearer* [2017], this does not prove self-similarity, and indeed better fits to the data can be obtained for five regions of dense seismicity in southern California if stress drop increases with moment in the Brune model, or if n is less than 2. The fundamental observation for southern California is that the larger earthquakes, on average, radiate more high-frequency energy than a self-similar Brune model predicts, within the available frequency range of the data. This can be explained in terms of simple circular source models either with higher stress drops for the larger events, or with a gentler HF falloff rate. Because of the interaction with the estimated global EGF function, the models with greater stress-drop scaling also have lower stress drops overall. Our synthetic tests suggest that these parameter tradeoffs are an important and often neglected aspect of stress drop studies. If these effects are not taken into account, then apparent differences in average stress drop between different studies or between different regions are not reliable.

Given the limited frequency range of the data, a gentler HF falloff could be from a less sharp corner in the source model, although this contrasts with the many studies using EGFs that find the steeper corner of the Boatwright model more appropriate [e.g. *Ruhl et al.*, 2017; *Huang et al.*, 2016]. Any slip heterogeneity in the earthquakes would also produce bumps in the spectra, which would bias the corner frequency from simple source modeling [e.g. *Ruhl et al.*, 2017; *Uchide and Imanishi*, 2016] and would affect the larger events more, as the bumps will likely be outside the frequency range of the data for the smaller events.

Our goal in future SCEC research is to quantify these tradeoffs and uncertainties in greater detail and devise strategies to minimize their impacts. Expanding the moment and frequency range of the data will certainly help, although it is unclear that this will make much difference except for specialized datasets, such as borehole records that record with good signal-to-noise at 100 Hz and above. Alternatively, it may be possible to stabilize the EGF calculation by limiting how much EGF functions can vary over short distances. This will at least expand the area over which valid relative comparisons between event stress drops are possible, even if their absolute values remain poorly constrained.

SCEC Related Publications (5 years) by Abercrombie and Shearer

Abercrombie, R. E., Ruhl, C. J., & Smith, K. D. (2017, 08). Detailed observations of seismicity, stress drop and directivity on a complex fault structure in Mogul Nevada. Poster Presentation at 2017 SCEC Annual Meeting. SCEC ID 7808

Abercrombie, R. E., Investigating uncertainties in empirical Green's function analysis earthquake source parameters, *J. Geophys. Res*., doi: 10.1002/2015JB011984, 2015. SCEC ID 8110.

Abercrombie, R. E., S. Bannister, J. Ristau and D. Doser, Variability of earthquake stress drop in a subduction setting, the Hikurangi Margin, New Zealand, *Geophys. J. Int*., doi:10.1093/gji/ggw393, 2017a. SCEC ID 7266

Abercrombie, R. E., Poli, P. & Bannister, S., Earthquake Directivity, orientation and stress drop within the subducting plate at the Hikurangi margin, New Zealand. *Journal of Geophysical Research: Solid Earth, 122*. https://doi.org/10.1002/2017JB014935, 2017b. SCEC ID 8112

Chen, X., and P. M. Shearer, California foreshock sequences suggest aseismic triggering process, *Geophys. Res. Lett*., **40**, doi:10.1002/grl.50444, 2013. SCEC ID 1775

Chen, X., and P. M. Shearer, Analysis of foreshock sequences in California and implications for earthquake triggering, *Pure Appl. Geophys.*, doi: 10.1007/s00024-015-1103-0, 2015. SCEC ID 8122

Chen, X., P. M. Shearer, and R. E. Abercrombie, Spatial migration of earthquakes within seismic clusters in Southern California: Evidence for fluid diffusion, *J. Geophys. Res.*, **117**, B04301, doi: 10.1029/2011JB008973, 2012. SCEC ID 1722

Goebel, T. H. W., E. Hauksson, P. M. Shearer, and J. P. Ampuero, Stress drop heterogeneity within tectonically complex regions: A case study of San Gorgonio Pass, southern California, *Geophys. J. Int*., **202**, 514–528, 2015. SCEC ID 6113

Hatch, R. L., Smith, K. D., & Abercrombie, R. E. (2017, 08). Analysis of Two Magnitude ~4 Earthquakes and Aftershocks Near Truckee, California, 2017. Poster Presentation at 2017 SCEC Annual Meeting. SCEC ID 7852

Hauksson, E., J Stock, R. Bilham, M. Boese, X. Chen, E. H. Fielding, J. Galetzka, K. W. Hudnut, K. Hutton, L. C. Jones, H. Kanamori, P. M. Shearer, J. Steidl, J. Treiman, S. Wei, and Wenzheng Yang, Report on the August 2012 Brawley earthquake swarm in Imperial Valley, Southern California, *Seismol. Res. Lett*., **84**, 177-189, doi: 10.1785/0220120169, 2013. SCEC ID 1678

Kane, D. L., P. M. Shearer, B. P. Goertz-Allmann, and F. L. Vernon, Rupture directivity of small earthquakes at Parkfield, *J. Geophys. Res.*, **118**, doi: 10.1029/2012JB009675, 2013. SCEC ID 1725

Kaneko, Y., and P. M. Shearer, Seismic source spectra and estimated stress drop from cohesive-zone models of circular subshear rupture, *Geophys. J. Int.*, doi: 10.1093/gji/ggu030, 2014. SCEC ID 1830

Kaneko, Y., and P. M. Shearer, Variability of seismic source spectra, estimated stress drop and radiated energy, derived from cohesive-zone models of symmetrical and asymmetrical circular and elliptical ruptures, *J. Geophys. Res*., **120**, doi: 10.1002/2014JB011642, 2015. SCEC ID 8120

Ruhl, C. J., Abercrombie, R. E., & Smith, K. D. (2017). Spatiotemporal Variation of Stress Drop During the 2008 Mogul, Nevada, Earthquake Swarm. *Journal of Geophysical Research: Solid Earth*, 122(10), 8163-8180. doi: 10.1002/2017JB014601. SCEC ID 8114.

Ruhl, C. J., R. E. Abercrombie, K. D. Smith, and I. Zaliapin, Complex Spatiotemporal Evolution of the 2008 M_w 4.9 Mogul Earthquake Swarm (Reno, Nevada): Interplay of Fluid and Faulting, *J. Geophys. Res.*, **121**, doi:10.1002/2016JB013399, 2016. SCEC ID 8113

Shearer, P. M., Self-similar earthquake triggering, Båth's law, and foreshock/aftershock magnitudes: Simulations, theory, and results for southern California, *J. Geophys. Res.*, **117**, B06310, doi: 10.1029/2011JB008957, 2012a. SCEC ID 1723

Shearer, P. M., Space-time clustering of seismicity in California and the distance dependence of earthquake triggering, *J. Geophys. Res.*, **117**, B10306, doi: 10.1029/2012JB009471, 2012b. SCEC ID 1724

Shearer, P. M., Reply to comment by S. Hainzl on "Self-similar earthquake triggering, Båth's Law, and foreshock/aftershock magnitudes: Simulations, theory and results for southern California," *J. Geophys. Res.*, **118**, doi: 10.1002/jgrb.50133, 2013. SCEC ID 6190

Shearer, P. M., Abercrombie, R. E., & Trugman, D. T. (2017, 08). Testing and Reconciling Stress Drop and Attenuation Models for Southern California. Poster Presentation at 2017 SCEC Annual Meeting. SCEC ID 7566

Sumiejski, P. E., and P. M. Shearer, Temporal stability of coda Q^{-1} in southern California, *Bull. Seismol. Soc. Am.*, **102**, 873–877, doi: 10.1785/0120110181, 2012. SCEC ID 8120

Trugman, D.T., P. M. Shearer, A. A. Borsa, and Y. Fialko, A comparison of long-term changes in seismicity at the Geysers, Salton Sea, and Coso geothermal fields, *J. Geophys. Res*., doi: 10.1002/2015JB012510, 2016. SCEC ID 8119

Trugman, D. T., and P. M. Shearer, GrowClust: A hierarchical clustering algorithm for relative earthquake relocation, with application to the Spanish Springs and Sheldon, Nevada, earthquake sequences, *Seismol. Res. Lett*., **88**, 1-13, doi: 10.1785/0220160188, 2017. SCEC ID 8118

Trugman, D. T., and P. M. Shearer, Application of an improved spectral decomposition method to examine earthquake source scaling in southern California, *J. Geophys. Res.*, **122**, 2890-2910, doi: 10.1002/2017JB013971, 2017. SCEC ID 7235

Trugman, D. T., and P. M. Shearer, Strong correlation between stress drop and peak ground acceleration for recent M 1–4 earthquakes in the San Francisco Bay area, *Bull. Seismol. Soc. Am*., **108**, 929-945, doi: 10.1785/0120170245, 2018. SCEC ID 8117

Uchide, T., H. Yao, and P. M. Shearer, Spatio-temporal distribution of fault slip and high-frequency radiation of the 2010 El Mayor-Cucapah, Mexico earthquake, *J. Geophys. Res.*, **118**, doi: 10.1002/jgrb.50144, 2013. SCEC ID 1774

Wang, W., and P. M. Shearer, Using direct and coda wave envelopes to resolve the scattering and intrinsic attenuation structure of Southern California, *J. Geophys. Res*., **122**, 7236-7251, doi: 10.1002/2016JB013810, 2017. SCEC ID 8116

Zhang, Q., and P. M. Shearer, A new method to identify earthquake swarms applied to seismicity near the San Jacinto Fault, California, *Geophys. J. Int*., **205**, 995-1005, doi: 10.1093/gji/ggw073, 2016. SCEC ID 6201

References

Abercrombie, R. E., S. Bannister, J. Ristau and D. Doser, Variability of earthquake stress drop in a subduction setting, the Hikurangi Margin, New Zealand, *Geophys. J. Int*., doi:10.1093/gji/ggw393, 2017a.

Abercrombie, R. E., Poli, P. & Bannister, S., Earthquake Directivity, orientation and stress drop within the subducting plate at the Hikurangi margin, New Zealand. *Journal of Geophysical Research: Solid Earth, 122*. https://doi.org/10.1002/2017JB014935, 2017b.

Baltay, A. S., T. C. Hanks and G. C. Beroza, Stable stress drop measurements and their variability: implications for ground-motion prediction. *Bull. Seism. Soc. Am., 103*, doi: 10.1785/0120120161, 2013.

Baltay, A. S., T. C. Hanks, and N. A. Abrahamson, Uncertainty, variability, and earthquake physics in ground-motion prediction equations, *Bull. Seismol. Soc. Am*. 107, 1754–1772, doi: 10.1785/ 0120160164, 2017.

Abercrombie, R. E. and Rice, J. R., Can observations of earthquake scaling constrain slip weakening?, *Geophys. J. Int., 162*, 406-424, 2005.

Brune, J., Tectonic stress and the spectra of seismic shear waves from earthquakes, *J. Geophys. Res., 75*, 4997-5009, 1970.

Cotton, F., R. Archuleta and M. Causse, What is the sigma of the stress drop? *Seismol. Res. Letts., 84*, 42-48, doi: 10.1785/0220120087, 2013.

Hauksson, E., Average Stress Drops of Southern California Earthquakes in the Context of Crustal Geophysics: Implications for Fault Zone Healing, *Pure Appl. Geophys*., 1–12,doi:10.1007/s00024-014-0934-4, 2014.

Hauksson, E., and P. M. Shearer, Attenuation models (Qp and Qs) in three dimensions of the southern California crust: Inferred fluid saturation at seismogenic depths, *J. Geophys. Res.*, **111**, B05302, doi:10.1029/2005JB003947, 2006.

Huang, Y., G. C. Beroza, and W. L. Ellsworth, Stress drop estimates of potentially induced earthquakes in the Guy-Greenbrier sequence, *J. Geophys. Res. Solid Earth*, *121*, 6597–6607, doi:10.1002/2016JB013067, 2016.

Kanamori, H. and E.E. Brodsky, The physics of earthquakes, *Reports on Progress in Physics*, **67**, 1429 - 1496, DOI:10.1088/0034-4885/67/8/R03, 2004.

Kaneko, Y., and P. M. Shearer, Seismic source spectra and estimated stress drop from cohesive-zone models of circular subshear rupture, *Geophys. J. Int.*, doi: 10.1093/gji/ggu030, 2014.

Kaneko, Y., and P. M. Shearer, Variability of seismic source spectra, estimated stress drop and radiated energy, derived from cohesive-zone models of symmetrical and asymmetrical circular and elliptical ruptures, *J. Geophys. Res*., **120**, doi: 10.1002/2014JB011642, 2015.

Kwiatek, G., Bulut, F., Bohnhoff, M., Dresen, G., High-resolution analysis of seismicity induced at Berlín geothermal field, El Salvador. - *Geothermics*, *52*, 98-111, doi: org/10.1016/j.geothermics.2013.09.008, 2014.

Kwiatek, G., K. Plenkers and G. Dresen, Source parameters of picoseismicity recorded at Mponeng deep gold mine, South Africa: implications for scaling relations. *Bull. Seism. Soc. Am., 101*, 2592-2608, doi: 18101/10.1785/0120110094, 2011.

Madariaga, R., Dynamics of an expanding circular crack, *Bull. Seism. Soc. Am., 66*, 639-666, 1976.

Oth, A., D. Bindi, S. Parolai and D. Di Giacomo, Spectral analysis of K-NET and KiK-net data in Japan, Part II: On attenuation characteristics, source spectra, and site response of borehole and surface stations. *Bull. Seismol. Soc. Am., 101*, 667-687, doi: 10.1785/0120100135, 2011.

Pacor, F., D. Spallarossa, A. Oth, L. Luzi, R. Puglia, L. Cantore, A. Mercuri, M. D'Amico and D. Bindi, Spectral models for ground motion prediction in the L'Aquila region (central Italy): evidence for stress drop dependence on magnitude and depth, *Geophys. J. Int. 204*, 697-718, doi:10.1093/gji/ggv448, 2016.

Ruhl, C. J., Abercrombie, R. E., & Smith, K. D. (2017). Spatiotemporal variation of stress drop during the 2008 Mogul, Nevada, earthquake swarm. *Journal of Geophysical Research: Solid Earth*, 122, 8163–8180. https://doi.org/10.1002/2017JB014601

Shearer, P. M., G. A. Prieto, and E. Hauksson, Comprehensive analysis of earthquake source spectra in southern California, *J. Geophys. Res.*, **111**, B06303, doi:10.1029/2005JB003979, 2006.

Trugman, D. T., and P. M. Shearer, Application of an improved spectral decomposition method to examine earthquake source scaling in southern California, *J. Geophys. Res.*, doi: 10.1002/2017JB013971, 2017.

Uchide, T., and K. Imanishi, Small Earthquakes Deviate from the Omega-Square Model as Revealed by Multiple Spectral Ratio Analysis, *Bull. Seism. Soc. Am., 106*, 1357–1363, doi: 10.1785/0120150322, 2016

Zhang, H., D. W. Eaton, G. Li, Y. Liu, and R. M. Harrington, Discriminating induced seismicity from natural earthquakes using moment tensors and source spectra, *J. Geophys. Res. Solid Earth, 121*, 972–993, doi:10.1002/2015JB012603, 2016,